MedChemComm

Accepted Manuscript

ROYAL SOCIETY OF CHEMISTRY

www.rsc.org/medchemcomm

Cite this: DOI: 10.1039/c0xx00000x

www.rsc.org/xxxxxx

ARTICLE TYPE

Targeted Photoresponsive TiO_2-Coumarin nanoconjugate for efficient Combination therapy in MDA-MB-231 breast cancer cells: Synergic effect of Photodynamic Therapy (PDT) and Anticancer drug Chlorambucil

Moumita Gangopadhyay,[a] Sourav K. Mukhopadhyay,[b] S. Karthik,[a] Shrabani Barman[a] and N. D. Pradeep Singh*[a]

Received (in XXX, XXX) Xth XXXXXXXXX 20XX, Accepted Xth XXXXXXXXX 20XX
DOI: 10.1039/b000000x

Coupling of photodynamic therapy (PDT) with chemotherapy is an emerging treatment modality because of its ability to improve the antitumor effect and reduce the toxicity of the anticancer agents. Metallic NPs, silica NPs and carbon nanotubes have become rising star as drug carriers for both photosensitizers and chemotherapeutic agents. But to date there are only few reports using the aforesaid NPs as a platform for PDT combined chemotherapy. Hence, we have developed a targeted metallic single nanoparticle system for the amalgamation of PDT with chemotherapy. The NPs for combination therapy have been constructed using two main ingredients: folic acid decorated TiO_2 NPs and coumarin chromophore. The newly synthesized coumarin chromophore performed three important roles (i) being a fluorophore for cell imaging (ii) photosensitizer for PDT (iii) a phototrigger for regulated anticancer drug release. Furthermore, folic acid decorated TiO_2 NPs help in internalization of drug inside the cancer cells. In vitro biological studies reveal that this targeted combination treatment results in an enhanced tumor accumulation of TiO_2 nanoparticles, significant inhibition to tumor cell proliferation and increased induction of apoptosis. Such metallic photoresponsive NPs which are benign to physiological system, permeate easily into cells and exhibits high therapeutic efficacy, will have significant prospective against drug-resistant tumors.

Introduction

The term "Combination therapy" refers to using multiple therapies to treat a *single* disease either by administering separate drugs or dosage forms containing more than one active ingredient to cause additive or even synergistic effect for enhanced therapeutic efficacy. Conditions treated with combination therapy includes tuberculosis, leprosy, cancer, malaria, HIV/AIDS, hypertension etc. Among these, cancer is one of the most pressing public health concerns of the 21st century. Now it is well known that Photodynamic therapy (PDT) is a well established therapy for the localized treatment of cancers because it renders spatial and temporal selectivity and specificity.[1] Several preclinical studies suggest that the use of PDT in combination with established treatments or with newly-developed modalities may be of great benefit as compared to the monotherapies. In particular, combination of PDT with chemotherapeutics can be employed synergistically to treat high-risk tumors with a goal of total tumor eradication.[2] Clearly positive results have been reported in experiments exploiting the combination of PDT with cisplatin,[3] doxorubicin,[4] mitomycin C,[5] for an enhanced cytotoxic and apoptotic effect. In all these studies, both the photosensitizer and the anticancer drug need to be colocalized in the tumor cell. One approach for achieving colocalization is to deliver both the photosensitizer and the anticancer drug simultaneously to the tumor cell using a delivery system that encapsulates both the agents.

In recent years nanoparticulate systems (NPs) for combination therapies for effective cancer treatment have been well explored since they have shown several unique features such as ratiometric drug loading, temporal drug release and targeted delivery, that are untenable in traditional chemotherapy.[6a] Two photon and NIR active NPs showed high prospect in this regard due to their negligible background autofluorescence and deep penetration ability.[6b]Accordingly, Liposomes, polymeric NPs and dendrimers have been explored as drug delivery vehicles for the combination of PDT and chemotherapy.[7] Currently, there has been surging interest on metallic NPs, silica NPs and carbon nanotubes as drug carriers for both photosensitizers and chemotherapeutic agents. But interestingly there has been only few reports using the above said NPs as a platform for combination of PDT and chemotherapy, mainly because of their less functionalizable nature.[6] To address the lack of synthetic flexibility in inorganic NPs, researchers synthesized hybrid inorganic NPs by decorating with polymers and demonstrated its ability for multidrug

encapsulation.[7] The synthesis of these hybrid inorganic NPs for dual drug delivery involves three crucial steps (i) loading of drug on the NPs by passive diffusion (ii) decoration of drug loaded NPs by the polymer and (iii) binding of the second drug on the polymer bounded NPs. [7] By any means, if we can design an organic molecule which can act as a photosensitizer and can also release a chemotherapeutic agent in presence of the same external stimulus light, then we can bypass the above mentioned crucial steps involved in the synthesis of hybrid inorganic NPs and utilize these NPs directly for combination therapy.

The basic requirement to construct targeted metallic NPs for PDT combined chemotherapy is to develop two essential ingredients: (i) chromophore which can act both as a photosensitizer and phototrigger, simultaneously (ii) tumor targeted biocompatible nanocarriers. For the current study, we selected coumarin derivatives as our chromophore since they have been reported to show PDT activity and phototrigger ability by both one and two-photon excitation, independently.[8,9] Further, we also chose folic acid decorated TiO_2 NPs as our nanocarriers because of their biocompatibility, enhanced cellular uptake and target ability. In the present work, we have constructed targeted combination therapeutic system using two main ingredients, folic acid decorated TiO_2 NPs and 7,8-dihydroxy coumarin chromophore for efficient destruction of MDA-MB breast cancer cells via the synergic effect of both PDT and well known chemotherapeutic drug chlorambucil as shown schematically in **Figure 1.**

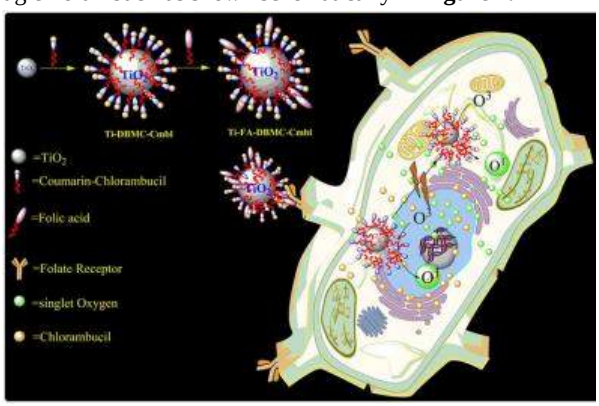

Figure 1 Schematic representation of the effect of combination therapy of folic acid decorated TiO_2 loaded with Coumarin-chlorambucil conjugate on cancer cells

2. Result and Discussion

2.1 Synthesis of TiO_2 NPs loaded with coumarin-chlorambucil (Ti-DBMC-Cmbl NPs)

We synthesized coumarin−chlorambucil conjugate (DBMC-Cmbl) (**4**)[10] by treating 7,8-dihydroxy-4-bromomethylcoumarin (**3**) with chlorambucil in presence of potassium carbonate in dry DMF at room temperature (**see SI, Figure S1-S2**). Later, we covalently anchored DBMC-Cmbl conjugate onto the surface of TiO_2 nanoparticles to afford Ti-DBMC-Cmbl NPs **(5)** by slow addition of KOH followed by TiO_2 nanoparticles into an ethanolic solution of DBMC-Cmbl (**Scheme 1)**. The reaction was carried out in inert and dark condition to avoid any degradation of the generating particles. Finally, the TiO_2 loaded DBMC-Cmbl was collected by centrifuge method and washed twice with acetone and dried under vacuum.

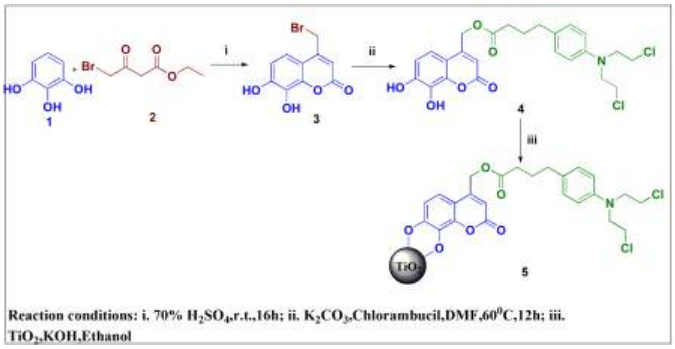

Scheme 1. Synthesis of Ti-DBMC-Cmbl NPs **(5)**

2.2. Characterization of Ti-DBMC NPs: Absorption, Emission and FTIR Spectral data

The attachment of DBMC-Cmbl on the surface of TiO_2 NPs was analyzed by FT-IR, UV–vis, and fluorescence spectroscopic methods. IR spectra of DBMC-Cmbl, TiO_2 NPs and Ti-DBMC-Cmbl NPs are shown in **Figure S3**. Disappearence of the characteristic phenolic O-H stretching frequency at 3200-3500 cm^{-1} of coumarin moiety and appearence of peaks between 500-600 cm^{-1} of Ti-O vibration [11] in the IR spectra of Ti-DBMC-Cmbl NPs, indicates covalent attachment of DBMC-Cmbl onto TiO_2 NP surface. Further, shift in C=O stretching frequency of coumarinyl cyclic ester of DBMC-Cmbl to lower frequency (1630 cm^{-1}) in case of Ti-DBMC-Cmbl NPs confirms the attachment of the DBMC-Cmbl on the TiO_2 surface.[12] The UV–vis and fluorescence spectra of Ti-DBMC-Cmbl NPs are presented in **Figure 2a & b** respectively. The Ti-DBMC-Cmbl NPs showed two absorption peaks at 250 and 330 nm due to π–π* and n–π* transitions of coumarin moiety respectively, and a new shoulder at around 500 nm due to binding of coumarin on the surface of TiO_2 NPs.[13] (**Figure 2a**). Further, Ti-DBMC-Cmbl NPs also showed good fluorescence with emission maxima at 430 nm similar to DBMC-Cmbl (**Figure 2b**).The fluorescence quantum yield of Ti-DBMC-Cmbl NPs was found to be 0.064 taking quinine sulphate as a standard (**Table S1**). Moreover, the TGA and solid state UV spectra also supported the loading of DBMC-Cmbl conjugate on TiO_2 NPs (**Figure S4-S5**). The amount of loading of DBMC-Cmbl conjugate on TiO_2 surface was calculated as 63.3µg/mg of TiO_2 (**Figure S6**).

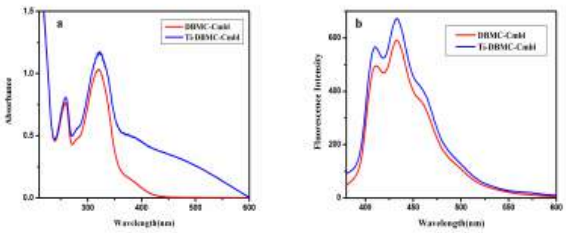

Figure 2 (a) Absorption and (b) Emission spectra of DBMC-Cmbl and Ti-DBMC-Cmbl NPs in ethanol

2.3 Size and Shape of Ti-DBMC-Cmbl NPs

The size and shape of the NPs were observed by the TEM study. The representative TEM image of Ti-DBMC-Cmbl NPs is presented in **Figure 3a. Figure 3a** shows that the NPs were aggregated and globular in nature with a particle size of ~100 nm. This size of the NPs is well within the preferred range of the NPs useful for effective drug-delivery. Further, DLS data showed that Ti-DBMC-Cmbl NPs had an average particle size of ~164.18 nm (**Figure 3b**), which is higher compared to the values obtained from TEM analysis.

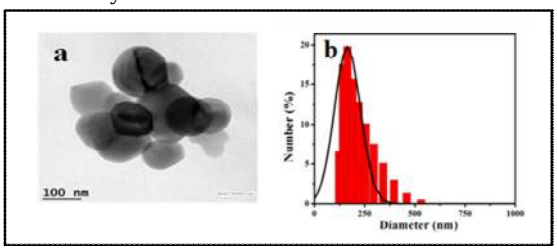

Figure 3 (a) TEM image and (b) Dynamic light scattering (DLS) spectra of Ti-DBMC-Cmbl NPs respectively

2.4 Evidence of PDT activity of Ti-DBMC-Cmbl NPs

2.4.1 Photoinduced DNA cleavage experiment [14]

To examine the PDT efficiency of Ti-DBMC-Cmbl NPs, we prepared chlorambucil-free coumarin derivative viz. 7,8-dihydroxy-4-methyl coumarin (DMC) and conjugated on TiO_2 NPs leading to the formation of Ti-DMC NPs **(See SI, section 4, Figure S7-S10)**, since chlorambucil has ability to induce DNA cleavage and might produce misleading results. Initially, we irradiated supercoiled circular pBR322 plasmid DNA in presence of Ti-DMC NPs by UV-vis light (≥410 nm). The gel electrophoresis results (**Figure 4)** showed that Ti-DMC NPs induced ~95% cleavage of supercoiled (SC) DNA to its nicked circular (NC) form II in D_2O (lane 5), which infers that the DNA cleavage process is mediated by singlet oxygen as D_2O greatly enhances singlet oxygen lifetime.[15]

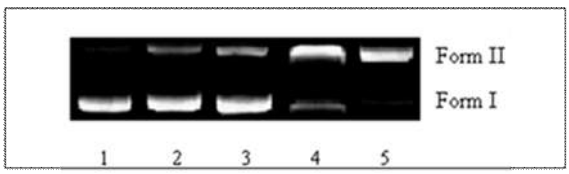

Figure 4 Single Strand DNA cleavage of supercoiled circular pBR322 DNA (Form I) to relaxed circular DNA (Form II) at ≥410nm with 10^{-4} (M) concentration; Lane 1: DNA, Lane 2: DNA+TiO_2 , Lane 3: DNA+DMC, Lane 4: DNA+Ti-DMC NPs, Lane 5: DNA+Ti-DMC+D_2O

To confirm the involvement of singlet oxygen in the DNA cleavage process, the photoinduced DNA cleavage experiments were performed in presence of various additives like NaN_3, D_2O and oxygen saturated solution. In O_2 saturated solution, the DNA cleaving ability of the Ti-DMC NPs was found to be higher than aerobic condition. In the solutions of Ti-DMC NPs purged with O_2, ~52.59% of form II DNA was generated whereas ~33.65% of form II DNA was noted in aerobic condition (**Figure 5**). Further the DNA cleavage efficiency of Ti-DMC NPs was also found to be greater in the presence of D_2O (~42.1% of form II DNA was produced). However in the presence of NaN_3, a well known singlet oxygen quencher,[16] the generated form II DNA by Ti-DMC NPs was found to be only ~23%. The above results suggested that singlet oxygen is playing the pivotal role in the DNA cleavage process. To examine the role of other reactive oxygen species like hydroxyl radicals in the DNA cleavage process, we carried out the experiment in presence of hydroxyl radical scavengers like DMSO,[17] which showed very little inhibitory effect in the DNA scission process (~32.06 % of form II DNA generated) **(Figure 5),** which indicated that hydroxyl radicals did not have much role in the DNA cleavage process. The mechanistic studies suggest that Ti-DMC NPs shows efficient PDT effect by producing singlet oxygen from molecular oxygen according to the Type II mechanistic pathway of PDT.

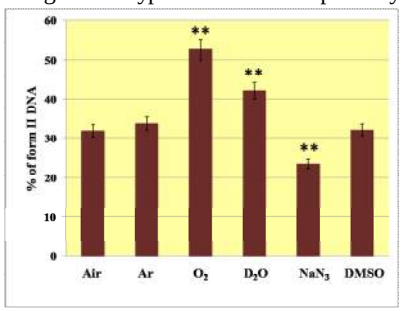

Figure 5 Bar diagram displaying the single strand cleavage of supercoiled circular pBR322 DNA (form I) to relaxed circular DNA (form II) by Ti-DMC particle(250 μg/mL) in presence of various additives in a sodium phosphate buffer (pH 7.0, 10 mM) ≥ 410 nm at room temperature for 30 min. Values are presented as means ± standard deviations of three different observations and significance level evaluated by comparing with the negative control using Student's t-test statistics: **P<0.01

2.4.2 Detection of singlet oxygen and measurement of singlet oxygen quantum Yield (Φ_Δ)[8]

We performed the well known photodegradation of 1,3-diphenylisobenzofuran (DPBF) in the presence of Ti-DMC NPs in order to detect the involvement of singlet oxygen. The decrease in absorbance of DPBF at 425 nm with respect to irradiation time in presence of Ti-DMC NPs, clearly proves the formation of singlet oxygen by the NPs **(Figure 6)**. The calculated singlet oxygen quantum yields (Φ_Δ) of the Ti-DMC NPs is found to be ~0.29 using TPP (Tetraphenylporphyrin) as reference having a known Φ_Δ of 0.68.

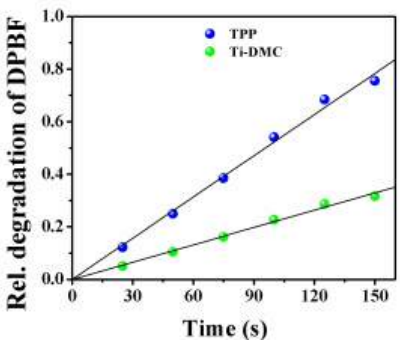

Figure 6 Photodegradation rate of DPBF in the presence of Ti-

DMC NPs and TPP at 425 nm

2.4.3 Photoinduced anticancer drug release by Ti-DBMC-Cmbl[18]

After successful demonstration of the PDT property of Ti-DBMC-Cmbl NPs, we investigated the photoinduced release of anticancer drug from Ti-DBMC-Cmbl NPs. For this purpose, photolysis of Ti-DBMC-Cmbl NPs was carried out. A suspension of Ti-DBMC-Cmbl NPs in aqueous acetonitrile was irradiated by UV-vis light (≥410 nm). The course of the photorelease of chlorambucil was followed by reverse phase HPLC (**Figure S11**). The HPLC profile indicates about 90% of the loaded anticancer drug (chlorambucil) was effectively released within 50 min of photolysis (**Figure 7a)**. Further, we also demonstrated precise control of the photolytic release of chlorambucil by monitoring the release of chlorambucil after periods of exposure to light and dark condition. The **Figure 7b** clearly shows that the drug release proceeded only under illumination. The photochemical quantum yield for the release was calculated as 0.034 (**Table S2**).

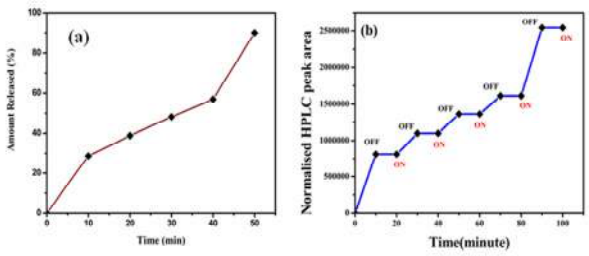

Figure 7 (a) Percentage of chlorambucil released from Ti-DBMC-Cbl.; (b) partial progress for the release of chlorambucil under bright and dark conditions."ON" indicates the beginning of light irradiation;"OFF" indicates the ending of light irradiation

2.5 Photophysical properties of Ti-DBMC-Cmbl

2.5.1 Fluorescence lifetime measurements[19,20]

In order to attain a deeper insight into the excited state properties of Ti-DBMC-Cmbl NPs, fluorescence lifetime has been recorded. **Figure 8** represents the time resolved fluorescence decay profile of DBMC-Cmbl and Ti-DBMC-Cmbl NPs. The decay behavior of the DBMC-Cmbl and Ti-DBMC-Cmbl NPs are found to be complicated and is best fitted to triexponential functions. It is interesting to note that the complicated triexponential decay pattern of the DBMC-Cmbl reflects the presence of a short-lived major component (~ 63 ps, ~ 43% in EtOH), which seems to be a representative of the lifetime of fluorophore undergoing rapid intersystem crossing to its excited triplet state which is consistent with literature.[8]

The decay behavior of Ti-DBMC-Cmbl NPs undergoes a noteworthy modification. Though the complicacy of the decay persists the overall increase of the average fluorescence lifetime of Ti-DBMC-Cmbl NPs is distinctly detectable (from ~3.8 ns to ~6 ns) which is not unlikely owing to the coupling of plasmonic absorption of the nanomaterial with the absorption of coumarin derivative which results in an increase in radiative rate constant. Further the short-lived major component (~ 60 ps) is also present here with an enhanced amplitude (~61%), which seems to be a representative of the enhanced rate of ISC stating the fact that the Ti-DBMC-Cmbl NPs are more effective photothera peutic agents than the bare DBMC-Cmbl.

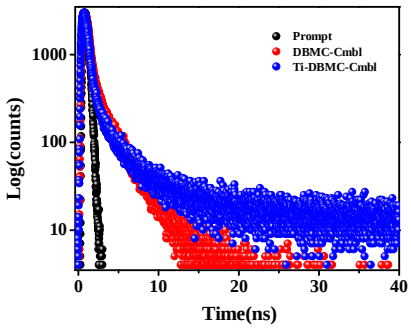

Figure 8 Single-photon counting of Ti-DBMC-Cmbl after excitation at 340 nm in ethanol solution

2.5.2 Transient absorption and Triplet state lifetime investigations[21,22]

For Ti-DBMC-Cmbl NPs, the transient species formed upon nanosecond time-resolved laser flash photolysis were investigated. The irradiation of the NPs at 350 nm in Ar-saturated and oxygen saturated ethanol solutions led to the transient spectra shown in **Figure 9**. The absorption band at 350 nm corresponds to the triplet-triplet absorption of the mentioned NPs. In both Ar-saturated and O_2-saturated ethanol, the transient decay of the NP follow first-order kinetics and lifetimes are found to be ~2.12 and ~1.70 μs respectively, which clearly corresponds to the efficient quenching of the triplet excited state of the NP by vestigial ground state molecular oxygen ($^3O_2$).[19]

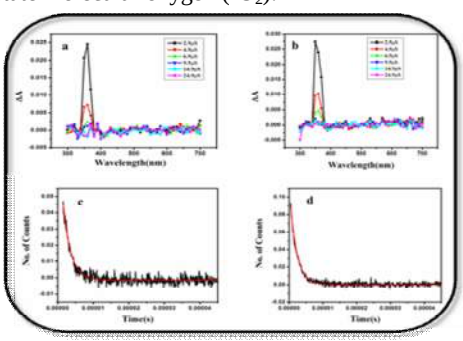

Figure 9 (a-b) Transient absorption spectra **(c-d)** Decay profile of triplet excited state of Ti-DBMC-Cmbl NPs in Ar and O_2 saturated ethanol, respectively

2.6 *In vitro* Cell cytotoxicity study of Ti-DBMC-Cmbl NPs

After the photochemical and photophysical studies, we were interested to observe the *in vitro* toxicity of the Ti-DBMC-Cmbl NPs against cancer cells. We evaluated cell viability using MTT assay in human breast cancer cell line MDA-MB-231. Cells were incubated with TiO_2, Ti-DMC, Ti-DBMC-Cmbl NPs and free drug chlorambucil separately for 4 h at a same concentration. After incubation, the cells were irradiated by UV-vis light (≥ 410 nm) and further incubated for 24 h.[23] As per our expectation, we observed enhanced cell cytotoxicity in case of Ti-DBMC-Cmbl NPs compared to both Ti-DMC NPs and Chlorambucil. From **Figure 10**, it is clearly noted that after 20 min of irradiation there

is a large increase of cell destruction for Ti-DBMC-Cmbl NPs as indicated by ~68% cell viability compared to ~78% cell viability for Ti-DMC NPs. Again, after 60 min of irradiation, only 35% of the cancer cells survived in case of Ti-DBMC-Cmbl NPs whereas ~ 64 % of cell viability was noted for Ti-DMC NPs. This larger tumor cell destruction of Ti-DBMC-Cmbl NPs can be attributed to the combined PDT and chemotherapeutic effect.

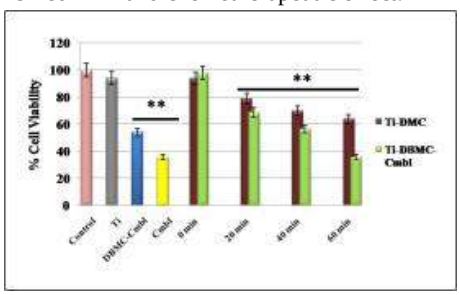

Figure 10 Comparative Cell viability study of Ti-DMC and Ti-DBMC-Cmbl NPs (250 µg/mL) on MDA-MB-231cell line after each 20 min of UV-vis irradiation (≥ 410 nm). TiO2 NPs, DBMC-Cmbl and Cmbl were also used in same concentration (250 µg/mL). Values are presented as means ± standard deviations of three different observations and significance level evaluated by comparing with the negative control using Student's t-test statistics: **P<0.01.

2.7 Cellular internalization of Ti-FA-DBMC-Cmbl NPs

To efficiently utilize our Ti-DBMC-Cmbl NPs for the cancer therapy, we functionalized our Ti-DBMC-Cmbl NPs with folic acid, as cancer cells are having folate receptors on their surfaces (**Scheme S2**).[24] Successful loading of folic acid (FA) on Ti-DBMC-Cmbl was achieved following literature known procedure and characterized by FTIR, UV/vis, Fluorescence, TGA, TEM, DLS studies (**Figure S12-S16)**. Thereafter, we studied cellular uptake efficiency of Ti-FA-DBMC-Cmbl NPs on MDA-MB-231 cells using confocal microscopy. **Figure 11** showed blue florescence (Excitation and emission maxima 405/461) and aggregation of Ti-FA-DBMC-Cmbl NPs in cell cytoplasm after 12 h of incubation followed by 60 min of irradiation under UV-vis light (≥410 nm).

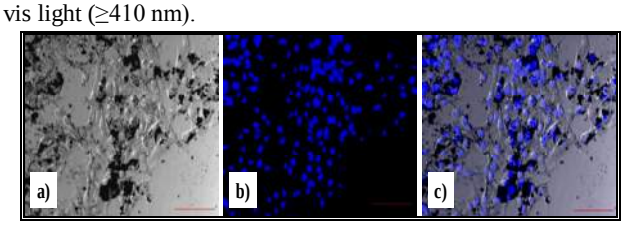

Figure 11 Real-time drug release studies using confocal microscopy. Shown are overlays of the bright-field image and the fluorescence images in the 461 nm emission channel after 60 min of photolysis. Scale bar =100µm.

2.7.2 Apoptosis induction and nuclear localization study of Ti-FA-DBMC-Cmbl NPs

To determine whether the NPs induced cell death is correlated with apoptosis, nuclear morphology of cells were assessed upon staining with DAPI.[25] Morphology of normal nuclei (smooth nuclear) and apoptotic nuclei (condensed or fragmented chromatin) was easily distinguished by this staining procedure. Nuclear condensation and fragmentation, one of the special features of apoptotic cell death, was seen in MDA-MB-231 cells which were incubated with Ti-FA-DBMC-Cmbl NPs and exposed to UV-vis light for 60 min (**Figure 12**). For further confirmation of apoptotic cell death by DNA damage, DNA fragmentation assay[26] was carried out. DNA fragmentation assay result showed presence of fragmented DNA (100-800 bp) in Ti-FA-DBMC-Cmbl NPs treated cells compared to control cell (lane 5, **Figure 12(c)**).

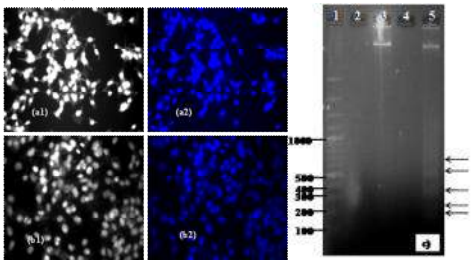

Figure 12 (A) DAPI staining; control cell nucleus (B) DAPI staining; Ti-FA-DBMC-Cmbl NPs (250 µg mL^{-1}) treated cell nucleus (C) DNA fragmentation assay. Lane 1: 100 bp DNA ladder (Fermentas); Lane 3: control MDA-MB-231 cell DNA; Lane 5: Ti-FA-DBMC-Cmbl nanoconjugate (250 µg mL^{-1}) treated MDA-MB-231 cell DNA; Lane 2, 4: Blank. Scale bar= 10µm.

On the other hand, a cellular uptake study after 12 h of incubation revealed that the Ti-FA-DBMC-Cmbl NPs were internalized by the cell leading to a uniform distribution of the sample inside the cell cytoplasm and nucleus as determined by PI staining.[27] In **Figure 13**, we noticed an overlap between the red fluorescence of PI and blue fluorescence of Ti-FA-DBMC-Cmbl NPs, which might indicate nuclear targeting ability of photoresponsive nanosystem. The blue fluorescence was evidently prevailing over the nucleus as well as surrounding the nucleus. Literatures regarding size dependence of NP-distribution in the sub-cellular level suggested that generally NPs of size >80 nm mostly resided near the nuclear membrane and could not enter into nucleus.[28] Ti-FA-DBMC-Cmbl NPs were having ~190 nm diameter. Hence, we can assume that the blue fluorescence inside the nucleus in **figure b3)** might be due to DBMC-Cmbl only as this moiety can leach out from the surface of TiO_2 NPs due to the acidic nature of various microenvironments inside the cell[29,30] and enter alone into the nucleus. Thus, from PI staining studies it can be inferred that the DBMC-Cmbl prodrug moiety might be diffusing into the nucleus after leaching out from the NP surface.

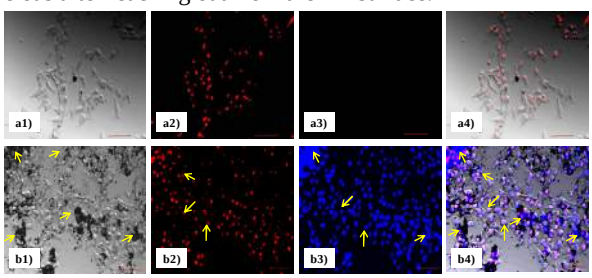

Figure 13 Nuclear localization studies using confocal

microscopy. Shown are (1) bright field images , fluorescence images (2) in the 625 nm (PI) and (3) 461nm (Ti-FA-DBMC-Cmbl NPs) emission channels and (4)overlays of the bright-field images and the fluorescence images; (A) untreated cells (b) cell treated with Ti-FA-DBMC-Cmbl NPs and after 60 min of photolysis. Scale bar =100 µm.

2.7.3 MTT Assay for Ti-FA-DBMC-Cmbl NPs

MTT assay revealed that Ti-FA-DBMC-Cmbl NPs showed efficient cytotoxicity against MDA-MB-231 breast cancer cell in comparison to either Ti-DBMC-Cmbl NPs or free Chlorambucil drug. Folic acid helps in efficient internalization of the Ti-DBMC-Cmbl NPs into the cancer cell resulting in greater accumulation of the NPs in the cell nucleus. From **Figure 14**, it is clearly seen that after 60 min irradiation there is a large increase of cell destruction for Ti-FA-DBMC-Cmbl NPs as indicated by only ~19% cell viability compared to ~35% cell viability for Ti-DBMC-Cmbl particles. Such enhanced damage of MDA-MB-231 breast cancer cell line was also monitored by cell cycle analysis described in **Figure S17 and Table S3.**

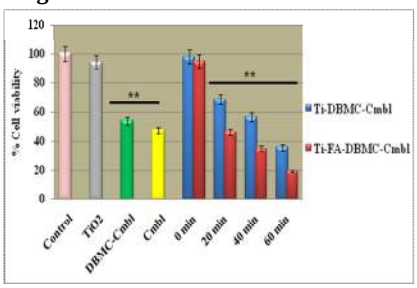

Figure 14 Comparative Cell viability Study of Ti-FA-DBMC-Cmbl and Ti-DBMC-Cmbl NPs (250 µg/mL) on MDA-MB-231cell line after regular time intervals of UV-vis irradiation (≥ 410 nm).). Values are presented as mean ± standard deviation of three different observations and significance level evaluated by comparing with the negative control using Student's t-test statistics: **P<0.01.

3. Experimental Section

3.1 Synthesis of TiO_2 NPs loaded with DBMC-Cmbl

Synthesis of Coumarin-Chlorambucil conjugate (DBMC-Cmbl)(4)

The phototrigger 7,8-dihydroxy-4-bromomethyl-chromen-2-one (DBMC) (**3**) was initially synthesized following the classical Pechmann condensation[10] as yellow solid in 80% yield, using pyrogallol (1 g, 8 mmol) and bromoethylacetoacetate (1.66 g, 8 mmol) as starting materials. Thereafter, the anticancer drug chlorambucil (0.097 g, 0.32 mmol) was coupled with 7,8-dihydroxy-4-bromomethyl coumarin (0.100g, 0.32 mmol) following previous report[23] from our group to afford DBMC-Cmbl (**4**) as yellow solid (70%); TLC R_f 0.6 (30% EtOAc in pet ether); ^{1}H NMR ($CDCl_3$, 200 MHz): δ = 7.39 (d, J = 8.2 Hz, 1H), 7.09(d, J = 8.4 Hz, 2H), 6.85 (d, J = 8.2 Hz, 1H), 6.64 (d, J = 8.4 Hz, 2H), 6.35 (s, 1H), 5.25 (s, 2H), 3.69−3.52 (m, 8H), 2.56−2.49 (t, J = 7.2 Hz, 2H), 2.43−2.36 (t, J = 7.4 Hz, 2H), 1.96−1.85 (m, 2H). ^{13}C NMR ($CDCl_3$, 50 MHz): δ = 173.6, 162.3, 155.3, 151.2, 145.3, 132.1, 129.3, 126.3, 114.3, 113.7, 111.2, 109.7, 62.6, 53.6, 40.6, 33.9, 33.7, 26.8. FTIR (KBr, cm^{-1}): 1720, 1622, 3210. UV−vis (solvent system: EtOH):λ_{max} (log ε): 330 (1.45). HRMS calcd For $C_{24}H_{25}Cl_2NO_5$ [MH+], 494.1137; found, 494.1134

Preparation of TiO_2 nanoparticle loaded with DBMC-Cmbl (Ti-DBMC-Cmbl NPs) (5)

10 mL of 10^{-4} (M) solution of DBMC-Cmbl (**4)** in dry ethanol was prepared. To it 2 equiv. of KOH pellets were added. Further, 0.100 g of prepared TiO_2 NPs was added under inert and dark condition with vigorous stirring. The reaction was monitored using UV/vis absorption spectroscopy, by collecting 0.1 mL aliquots from the reaction mixture at every 15 min interval. After completion of the reaction, the reaction mixture was diluted by 3 mL of ethanol. TiO_2 NPs loaded with DBMC-Cmbl were collected by centrifuging the diluted reaction mixture. The resultant Ti- DBMC-Cmbl NPs (**5**) were characterized by IR, UV/vis spectroscopy, fluorescence spectra, TGA, DLS and TEM images, solid state UV spectra.

3.2 Evidence for PDT activity

3.2.1 Procedure for DNA cleaving ability of Ti-DMC NPs[14]

To 10^{-4} M ethanolic solutions of each compounds viz. TiO_2, DMC and Ti-DMC was added same volume of pBR322 DNA (form I) solution from a stock of 62.5 µg/mL DNA in sodium phosphate buffer (10 mM, pH 7.0). Thus prepared solutions of TiO_2 + DNA, DMC+DNA and Ti-DMC+DNA were further exposed to UV-vis light of ≥410 nm at room temperature under aerobic conditions for 30 min, individually. After irradiation, each reaction mixture was stained with bromophenol blue and loaded on 1% agarose gel. Thereafter, the gel electrophoresis experiment was carried out using tank buffer (1X TAE) and GEL LOGIC 200 Imaging System was used for taking the image of the gel.

3.2.2 Photoinduced DNA cleavage of Ti-DMC NPs by adding different additives

To investigate the behavior of Ti-DMC NPs as photosensitizer i.e. to establish the role of singlet oxygen in the pBR322 DNA cleavage, the DNA cleavage experiments were carried out by adding different additives like D_2O (4 µL),[15] singlet oxygen scavenger NaN_3 (150 mM),[16] hydroxyl radical scavenger DMSO (4 µL),[17] in a 250 µg/mL solution of Ti-DMC NPs in sodium phosphate buffer solution. Thereafter, each of the Ti-DMC solution containing different additives were irradiated by UV-vis light (≥410 nm) at room temperature under aerobic condition for 30 min. After irradiation, each reaction mixture was stained with bromophenol blue and loaded on 1% agarose gel. Thereafter, the gel electrophoresis experiment was carried out using tank buffer (1X TAE). Afterwards, GEL LOGIC 200 Imaging System was used for taking the image of the gel.

3.2.3 Detection of Singlet oxygen[8]

In order to confirm the generation of singlet oxygen by Ti-DMC NPs, we recorded the photodegradation rate of 1,3-diphenylisobenzofuran(DPBF, Aldrich) in presence of the NPs. The singlet oxygen quantum yield (Φ_Δ) was determined using Tetraphenylporphyrin (TPP) as the reference having a singlet oxygen quantum yield of 0.68 in toluene. A mixed solution of the Ti-DMC NPs and DPBF (1,3-Diphenylisobenzofuran) were

prepared. In the solution, the concentration of the Ti-DMC NPs were adjusted to possess the same absorbance (~ 0.2) at 532 nm and the initial concentration of DPBF was maintained at 0.1 mM in all the cases. During the experiment, the solution was stirred vigorously to ensure the saturation of air. The solutions were then irradiated by an ND:YAG laser (Continuum-Surelite) and the photobleaching of the absorption band of DPBF at 425 nm was monitored using a photodiode (IP-28) and the output was processed using a Tektronix-TDS-2012B oscilloscope. The solution of DPBF alone was also irradiated and the obtained result was subtracted to diminish the errors originated from the photoactive compound itself. The Φ_Δ of the photosensitizers was calculated by the following simple equation:

$$\Phi_S = \frac{K_S}{K_R} \times \Phi_R \qquad (1)$$

Where, K is the slope of the photodegradation plot of DPBF against time (s) and the subscripts S and R denote the sample and the reference respectively and Φ_R is the singlet oxygen quantum yield of the reference (TPP).

3.3 Evidence for Photoinduced Anticancer Drug release from Ti-DBMC-Cmbl NPs

3.3.1 Photochemical properties of Ti-DBMC-Cmbl [18]

To monitor the controlled release of anticancer drug chlorambucil from Ti-DBMC-Cmbl particles, a dispersion of 30 mg NPs in 5 mL mixture of 90:10 acetonitrile/water was exposed to UV-vis light (≥410 nm) using 10% $NaNO_2$ solution in Millipore water as filter under N_2 atmosphere for 60 min. A medium pressure Hg lamp of 125 W powers was used as the light source. A 100 µL aliquot of the solution was collected after each 10 min. The clear supernatant solutions, obtained after centrifuging, were then passed through reversed-phase HPLC using acetonitrile as mobile phase. Flow rate was maintained at 1 mL/min.

3.3.2 Photophysical properties of Ti-DBMC-Cmbl

Fluorescence lifetime measurement [19,20]

For the investigation of the excited state properties of the Ti-DBMC-Cmbl NPs, fluorescence lifetime measurements were carried out with the help of Time Correlated Single-Photon counting (TCSPC) method. The experimental details are elaborated in the supporting information (**Section 3.1.(iii)**).

Triplet State lifetime measurement [21,22]

To assess the characteristics of transient species formed from Ti-DBMC-Cmbl NPs. Laser flash photolysis experiment was carried out using a nanosecond flash photolysis set-up (Applied Photophysics). Instrumental details and experimental procedure is explained in supporting information (**section 3.1.(iv)**).

3.4 *In vitro* Cell cytotoxicity studies using MDA-MB-231 cell line

3.4.1 MTT assay of Ti-DBMC-Cmbl NPs

Human breast adenocarcinoma (MDA-MB-231) cell lines were purchased from National Centre for Cell Science, Pune, India and were maintained in Dulbecco's Modified Eagle's medium (DMEM) supplemented with 10% fetal bovine serum. Cytotoxicity of Ti-DBMC-Cmbl NPs under dark as well as upon exposure to light on MDA-MB-231 cells was determined by conventional MTT assay. The exponential growth phase of the cells were trypsinised and seeded in 96-well flat-bottom culture plates at a density of 10^5 cells per well in 200 µL of DMEM complete medium. The cells were allowed to adhere and grow for 24 h at 37 °C in an incubator. The medium contained 180 µL fresh incomplete medium having 20 µL phosphate buffer saline (PBS), Ti, Ti-DMC NPs, Ti-DBMC-Cmbl NPs separately. Chemically treated cells were then irradiated with UV-vis radiation of ≥ 410 nm (0-60 min) and further incubated for about 24-48 h at 37 °C. [23] Following treatment for 24 and 48 h at 37°C, MTT solution (5mg/ml in PBS) was added and incubation was prolonged for 5 h at 37°C. Inhibition of cell proliferation was monitored by MTT (Himedia) assay.[31] Absorbance of the MTT-formazan product dissolved in DMSO (Himedia) was estimated at 595 nm using an ELISA plate reader (Thermo, USA). The inhibition of cell viability was calculated using the formula in equation **(2):**

$$\text{Inhibition}(\%) = \frac{\text{Absorbance(untreated cells)} - \text{Absorbance(treated cells)}}{\text{Absorbance(untreated cells)}} \qquad (2)$$

3.5 Cell imaging and Nuclear localization study of folic acid (FA) attached Ti-DBMC-Cmbl NPs (Ti-FA-DBMC-Cmbl)

3.5.1 Cell imaging study of Ti-FA-DBMC-Cmbl NPs

To study the cellular uptake of Ti-FA-DBMC-Cmbl NPs, briefly MDA-MB-231 cells (10^5cells/well) were anchored on 12-well plates and maintained there for 4−8 h. Thereafter, Ti-FA-DBMC-Cmbl treated cells were exposed to UV-vis light (≥410 nm) for 60 min at room temperature and were further incubated for another 12 h in presence of 5% CO_2. Next, the cells were treated with parafomaldehyde for a period of 15 min. After washing two times with PBS saline buffer the cells were visualized by Olympus FV1000 confocal microscope.[32]

3.5.2 Nuclear localization study of Ti-FA-DBMC-Cmbl NPs

DAPI staining for nuclear morphology observation

DAPI staining for nuclear morphology observations was performed as described by Uthaisang and co-workers.[25] MDA-MB-231 (10^5cells/well) cells were treated with the Ti-FA-DBMC-Cmbl NPs for 12 h after 60 min irradiation of UV-vis light of ≥410 nm along with the control (PBS). Then, cells were rinsed with phosphate buffer saline (PBS) and fixed in pretreatment solution for 5 min. Cells were incubated for 30 min with 1 mg mL^{-1} of 4', 6-diamidino-2-phenylindole (DAPI, Sigma) staining solution. DNA alterations like condensation or fragmentation were observed by fluorescence microscope (IX 51, Olympus) high-performance CCD camera using Image-Pro discovery 5.1 software.

DNA Fragmentation assay

Cleavage of DNA into oligonucleosomal fragments, recognizable as a DNA ladder when electrophoresed on an agarose gel, is usually considered as the biochemical hallmark of apoptosis.[26] Genomic DNA was isolated using quick Apoptotic DNA Ladder detection Kit (Invitrogen). Briefly, Ti-FA-DBMC-Cmbl NPs treated (60 min) and untreated MDA-MB-231 cells (10^5cells/well) were washed twice with 1X PBS. DNA was isolated from both treated and untreated cell by quick Apoptotic DNA Ladder detection Kit (Invitrogen), as per manufacturer protocol. Test Samples along with 100bp DNA ladder were loaded to 1% agarose gel and run with 50V for 2 h. DNA fragments were visualized using UV transilluminator (UST-20M-8R, Biostep, Germany).

Nuclear localization study of Ti-FA-DBMC-Cmbl NPs by PI staining

To study the nuclear targeting of Ti-FA-DBMC-Cmbl NPs, briefly MDA-MB-231 cells (10^5cells/well) were anchored on 12-well plates and maintained there for 4−8 h. Thereafter, Ti-FA-DBMC-Cmbl treated cells were exposed to visible light of ≥410 nm for 60 min at room temperature and were further incubated for another 12 h in presence of 5% CO_2. Next, the cells were treated with parafomaldehyde for a period of 15 min. After washing two times with PBS saline buffer the cells were stained with propidium iodide (40 µg/mL), and visualized by Olympus FV1000 confocal microscope.[27]

3.6 Cell cycle analysis of Ti-FA-DBMC-Cmbl NPs

In a similar manner as described for Ti-DBMC-Cmbl in Section 3.4.1, the in vitro cytotoxicity of Ti-FA-DBMC-Cmbl was also carried out via MTT assay and cell cycle ananlysis (Supporting Information **Table S3, figure S16**).

4. Conclusion

In conclusion, developed single nanoparticle system Ti-DBMC-Cmbl of ~164 nm size showed improved cytotoxicity to the MDA-MB-231 breast cancer cell line making use of dual therapeutic modalities such as PDT and phototriggered anticancer drug release. The PDT activity of the NPs was found to be moderately good with a singlet oxygen quantum yield value of 0.29. Also, the Ti-DBMC-Cmbl NPs showed ~90% drug release property after 60 min of irradiation with UV-vis light of ≥ 410nm wavelength. The singlet state as well as the triplet state lifetimes of the photoresponsive NPs are found to be ~6 ns and ~1.7 µs respectively, which supports the photosensitizing property of these NPs. We also introduced Folic acid on the surface of the particle to ensure targeted and enhanced cell damage. In vitro biological studies revealed that combination treatment by our developed NPs resulted in enhanced tumor accumulation, significant inhibition of tumor cell proliferation and increased induction of apoptosis. We also showed cellular internalization and nuclear localization studies of the NPs to emphasize on the apoptotic cell death. Thus, for the first time we synthesized an efficient targeted single photoresponsive nanosystem for competent combination therapy of cancer treatment. Hence, we expect our current findings to be a promising pioneer for utilizing variety of other NPs viz. NIR active NPs for such single component combination therapy as they will provide deeper penetration into tumor tissues.

Acknowledgement

We thank DST–SERB for sponsorship and DST FIST for 400 MHz NMR. Authors sincerely acknowledge Mr. Aniruddha Ganguly, Department of Chemistry, University of Calcutta for fluorescence lifetime measurements and singlet oxygen detection experiment. Authors also greatly acknowledge Professor Samita Basu, Chemical Science Division, Saha Institute of Nuclear Physics, Kolkata for triplet state lifetime measurements. Moumita is thankful to IIT Kharagpur for fellowship.

Notes and references

[a]*Department of Chemistry, Indian Institute of Technology Kharagpur 721302, West Bengal, India E-mail:ndpradeep@chem.iitkgp.ernet.in*
[b]*Department of Biotechnology, Indian Institute of Technology Kharagpur 721302, West Bengal, India*

† Electronic Supplementary Information (ESI) available: Details of spectral data analysis and synthesis are included in the ESI.

1 (a) J.P. Celli, B.Q. Spring, I. Rizvi, C.L. Evans, K.S. Samkoe, S. Verma, B.W. Pogue, T. Hasan, *Chem Rev*. 2010, **110**, 2795; (b) C.S. Foote, *Photochem. Photobiol*. 1991, **54**, 659; (c) S. Hatz, J.D. Lambert, P.R. Ogilby, *Photochem. Photobiol. Sci*. 2007, **6**, 1106.
2 I. Postiglione, A. Chiaviello, G. Palumbo, *Cancers* 2011, **3**, 2597
3 (a) M. Nonaka, H. Ikeda, T. Inokuchi, *Cancer Lett.* 2002, **184**, 171; (b) C. Compagnin, M. Mognato, L. Celotti, G. Canti, G. Palumbo, E. Reddi, *Cell Prolif.* 2010, **43,** 262; (c) C. Lottner, R. Knuechel, G. Bernhardt, H. Brunner, *Cancer Lett.* 2004, **203**, 171.
4 (a) A. Casas, H. Fukuda, P. Riley, A.M. del C Batlle, *Cancer Lett*. 1997, **121**, 105; (b) G. Canti, A. Nicolina, R. Cubeddu, P. Taroni, G. Bandieramonte, G. Valentini, *Cancer Lett.* 1998, **125**, 39; (c) J.G. Shiah, Y. Sun, C.M. Peterson, R.C. Straight, J. Kopecek, *Clin. Cancer Res*. 2000, **6**, 1008; (d) V. Kirveliene, G. Grazeliene, D. Dabkeviciene, I. Micke, D. Kirvelis, B. Juodka, J. Didziapetriene, *Cancer Chemother. Pharmacol*. 2006, **57**, 65.
5 I.P.J. van Geel, H. Oppelaar, Y.G. Oussoren, J.J. Schuitmaker, F.A. Stewart, *Br. J. Cancer* 1995, **72**, 344.
6 (a) C.M.J. Hu, S. Aryal, L. Zhang, *Therapeutic Delivery*, 2010**, 1**, 323; (b) J. V. Frangioni, *Curr. Opin. Chem. Biol.* 2003, **7**, 626.
7 C.M.J. Hu, L. Zhang, *Biochemical Pharmacology*, 2012, **83**, 1104
8 Q Zou, I. Zou, Y. Fang, Y. Zhao, H. Zhao, Y. Wang, Y. Gu, F. Wu, *J. Med. Chem*. 2013, **56,** 5288.
9 Q. Lin, Q. Huang, C. Li, C. Bao, Z. Liu, F. Li, L. Zhu, *J. Am.Chem. Soc*. 2010, **132**, 10645.
10 H.V. Pechmann, C. Duisberg, *Chem. Ber*. 1883**, 16**, 2119.
11 Y. Gao, Y. Masuda, Z. Peng, T. Yonezawa, K. Koumoto, *J. Mater. Chem*. 2003, **13,** 608.
12 S.T. Martin, J. K essselman, D.S. Park, N.S. Lewis, M.R. Hoffmann, *Environ. Sci. Technol.* 1996, **30,** 2535.
13 W.R. Duncan, O.V. Prezhdo, *J. Phys. Chem. B* 2005, **109,** 365.
14 N. Chowdhury, S. Dasgupta, N.D.P. Singh, *Bioorg. Med. Chem. Lett.*, 2012, **22**, 4668.
15 (a) A. U. Khan, *J. Phys. Chem*., 1976, **80**, 2219; (b) P.B. Merkel, D.R. Kearns, *J. Am. Chem. Soc*. 1972, **94**, 1029.
16 (a) G. Deby-Dupont, C. Deby, A. Mouithys-Mickalad, M. Hoebeke, L. Jadoul, A. Vandenberghe, M. Lamy, *Biochim. Biophys. Acta*, 1998, **1379**,

61; (b) J.R. Hwu, C.C. Lin, C.H. Chuang, K.Y. King, T.R. Su, S.C. Tsay, *Bioorg. Med. Chem*. 2004, **12**, 2509.
17 A. Hussain, S. Gadadhar, T.K. Goswami, A.A. Karande, A.R. Chakravarty, *Dalton Trans*. 2012, **41**, 885.
18 A. Jana, S. Atta, S.K. Sarkar, N.D.Pradeep Singh, *Tetrahedron*, 2010**, 52,** ,9798.
19 A. Ganguly, B.K. Paul, S. Ghosh, S. Kar, N. Guchhait, *Analyst*, 2014, **16**, 8465.
20 A. Ganguly, S. Jana, S. Ghosh, S. Dalapati, N. Guchhait, *Spectrochim. Acta Part A*, 2013**, 112**, 237.
21 H.Y. Yang, Z. Zhang, Z. H. Han, S.D. Yao, *Dyes and Pigments*, 2000**, 46**, 139.
22 M. K. Sarangi, S. Basu, *Phys. Chem. Chem. Phys.*, 2011, **13,** 16821.
23 S. Karthik, N. Puvvada, K.B.N. Prashanth, S. Rajput, A. Pathak, M. Mandal, N.D.P. Singh, *Applied material and interfaces*, 2013, **5**, 5232.
24 H. Chen, R. Ahn, J.V.d. Bossche, D.H. Thompson, T.V. O'Halloran, *Mol Cancer Ther* , 2009, **8**, 1955.
25 W. Uthaisang, D. Reutrakulb, B. Krachangchaeng, C. Fadeel, *Cancer Lett* 2004**, 208**, 171.
26 H.Y. Hsu, K.F. Hua, C.C. Lin, C.H. Lin, J. Hsu, C.H. Wong, *The Journal of Immunology* 2004**, 173**,5989.
27 T. Suzuki, K. Fujikura, T. Higashiyama, K. Takata, *The Journal of Histochemistry & Cytochemistry* 1997**, 45**, 49.
28. P. O. Andersson, C. Lejon, B. E. Hammarström, C. Akfur, L. Ahlinder, A. Bucht, L. Österlund, *Small* 2011, **7**, 514.
29. H. Zhang, C. W., B. Chen, X. Wang, *International Journal of Nanomedicine*, 2012, **7**, 235.
30. H. Zhang, B. Chen, H. Jiang, C. Wang, H. Wang, X. Wang, *Biomaterials*, 2011, **32**, 1906.
31. T. Mosmann, *J Immunol Methods* 1983, **65**, 55.
32. M. Pilatova, L. Varinska, P. Perjesi, M. Sarissky, L. Mirossay, P. Solar, A. Ostro, J. Mojzis, *Toxicol. In Vitro* 2010, **24**, 1347.

TOC

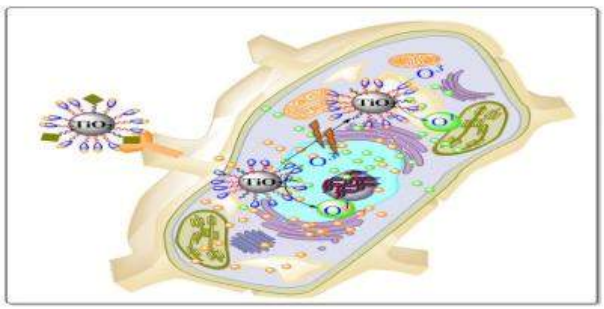

We have developed for the first time excellent targeted metallic single component nanoparticle system for combination of PDT and chemotherapy.